

How many explosions does one need? Quantifying supernovae in globular clusters from iron abundance spreads

**Henriette Wirth, Tereza Jerabkova, Zhiqiang Yan, Pavel Kroupa,
Jaroslav Haas and Ladislav Šubr**

March 14, 2022

Table of Contents

- 1 Introduction
- 2 Iron in globular clusters
- 3 The number of SNe
- 4 The time SF ends
- 5 Summary

Introduction

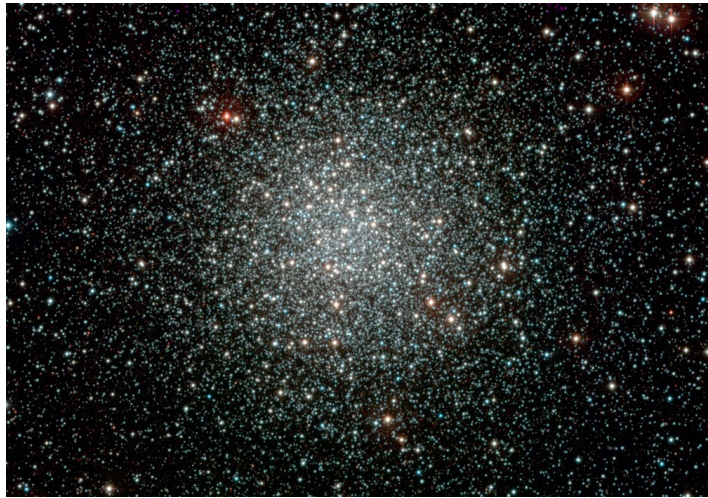


Figure: NGC 3201, obtained with the WFI instrument on the ESO/MPG 2.2-m telescope at La Silla, Credit:ESO

Introduction

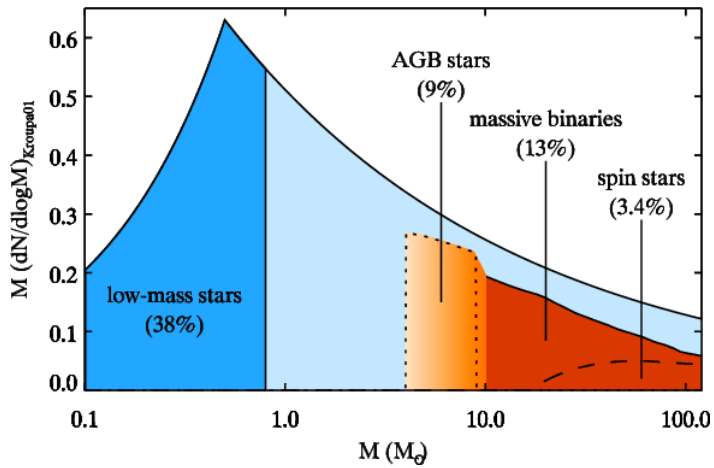


Figure: The IMF with different polluters and their mass fractions (Cottrell & Da Costa, 1981; Decressin et al., 2007; D'Ercole et al., 2008; de Mink et al., 2009; Wang et al., 2020).

Iron in globular clusters

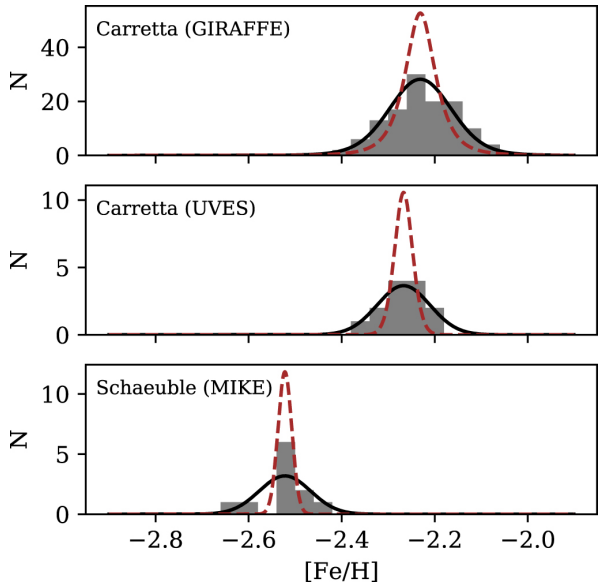


Figure: The iron abundances of stars in NGC 4590 from three different surveys (Bailin, 2019).

Iron in globular clusters

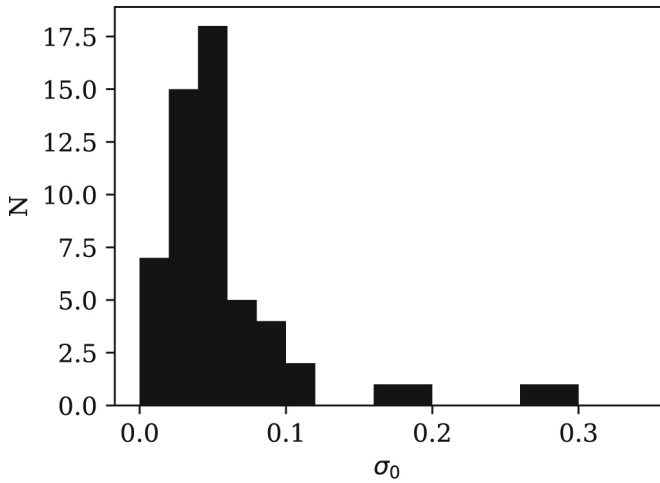


Figure: The iron abundance spread for 55 Milky Way GCs (Bailin, 2019).

The number of SNe

Wirth et al. (2021):

$$M_{\text{iron}} = p_{\text{iron}, \odot} \left(10^{[Fe/H] + \sigma_{[Fe/H]}} - 10^{[Fe/H] - \sigma_{[Fe/H]}} \right) \times M_{\text{ini}} \left(\frac{1}{\epsilon} - 1 \right)$$

The number of SNe

Wirth et al. (2021):

$$M_{\text{iron}} = p_{\text{iron}, \odot} \left(10^{[\text{Fe}/\text{H}] + \sigma_{[\text{Fe}/\text{H}]}} - 10^{[\text{Fe}/\text{H}] - \sigma_{[\text{Fe}/\text{H}]}} \right) \times M_{\text{ini}} \left(\frac{1}{\epsilon} - 1 \right)$$

The number of SNe

Wirth et al. (2021):

$$M_{\text{iron}} = p_{\text{iron}, \odot} \left(10^{[Fe/H] + \sigma_{[Fe/H]}} - 10^{[Fe/H] - \sigma_{[Fe/H]}} \right) \times M_{\text{ini}} \left(\frac{1}{\epsilon} - 1 \right)$$

The number of SNe

Wirth et al. (2021):

$$M_{\text{iron}} = p_{\text{iron}, \odot} \left(10^{[Fe/H] + \sigma_{[Fe/H]}} - 10^{[Fe/H] - \sigma_{[Fe/H]}} \right) \times M_{\text{ini}} \left(\frac{1}{\epsilon} - 1 \right)$$

The number of SNe

Wirth et al. (2021):

$$M_{\text{iron}} = p_{\text{iron}, \odot} \left(10^{[Fe/H] + \sigma_{[Fe/H]}} - 10^{[Fe/H] - \sigma_{[Fe/H]}} \right) \times M_{\text{ini}} \left(\frac{1}{\epsilon} - 1 \right)$$

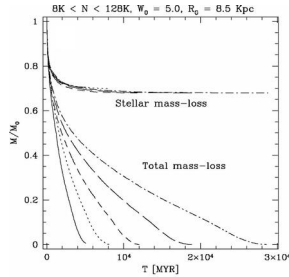
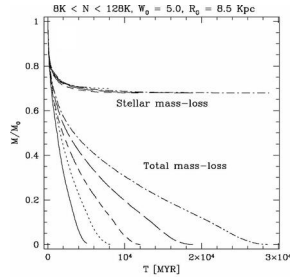


Figure: Mass loss of GCs based on N-Body simulations (Baumgardt & Makino, 2003).

The number of SNe

Wirth et al. (2021):

$$M_{\text{iron}} = p_{\text{iron}, \odot} \left(10^{[Fe/H] + \sigma_{[Fe/H]}} - 10^{[Fe/H] - \sigma_{[Fe/H]}} \right) \times M_{\text{ini}} \left(\frac{1}{\epsilon} - 1 \right)$$



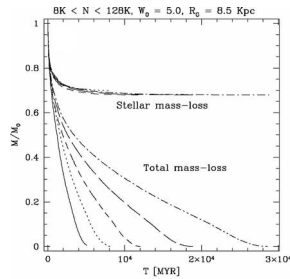
$$\rightarrow 0 = \beta \left[\frac{\frac{M_{\text{ini}}}{\langle m \rangle}}{\ln(\gamma \frac{M_{\text{ini}}}{\langle m \rangle})} \right]^x \frac{R_{\text{ap}}}{\text{kpc}} (1-e)^{\frac{1 - \frac{M(t)}{PSE M_{\text{ini}}}}{\frac{t}{\text{Myr}}}} - 1$$

Figure: Mass loss of GCs based on N-Body simulations (Baumgardt & Makino, 2003).

The number of SNe

Wirth et al. (2021):

$$M_{\text{iron}} = p_{\text{iron}, \odot} \left(10^{[Fe/H] + \sigma_{[Fe/H]}} - 10^{[Fe/H] - \sigma_{[Fe/H]}} \right) \times M_{\text{ini}} \left(\frac{1}{\epsilon} - 1 \right)$$



$$\rightarrow 0 = \beta \left[\frac{\frac{M_{\text{ini}}}{\langle m \rangle}}{\ln(\gamma \frac{M_{\text{ini}}}{\langle m \rangle})} \right]^x \frac{R_{\text{ap}}}{\text{kpc}} (1-e)^{\frac{1 - \frac{M(t)}{PSE M_{\text{ini}}}}{\frac{t}{\text{Myr}}}} - 1$$

Maoz & Graur (2017):

Figure: Mass loss of GCs based on N-Body simulations (Baumgardt & Makino, 2003).

$$m_{\text{SN}} = 0.074 M_{\odot}$$

The number of SNe

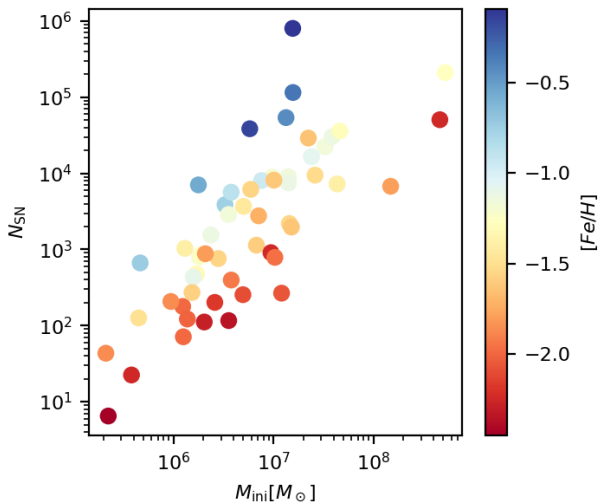


Figure: The number of SNe needed over the initial, colorcoded for the mean iron abundance (Wirth 2022 in submission).

The time SF ends

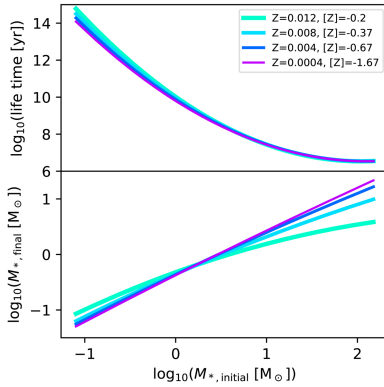


Figure: The life time and remnant mass of stars based on their initial mass(Yan et al., 2019).

The time SF ends

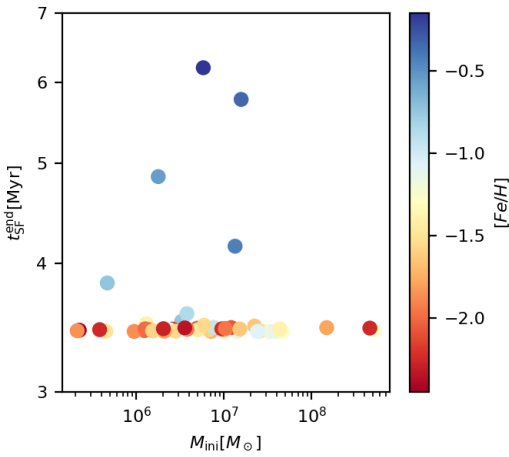


Figure: The time after which SF ends (Wirth et al. 2022 in submission). The empty dots are the solution using the canonical IMF the filled ones assume a top-heavy one.

Summary

- multiple populations of stars with different metallicities exist in GCs
- iron abundance spreads exist in some of them
- up to 10^5 SNe per GC (excluding Terzan 5)
- SF ends after $\sim 3.5 - 4$ Myr

References

- Bailin J., 2019, ApJS, 245, 5
- Baumgardt H., Makino J., 2003, MNRAS, 340, 227
- Calura F., Few C. G., Romano D., D'Ercole A., 2015, ApJ, 814, L14
- Cottrell P. L., Da Costa G. S., 1981, ApJ, 245, L79
- D'Ercole A., Vesperini E., D'Antona F., McMillan S. L. W., Recchi S., 2008, MNRAS, 391, 825
- Decressin T., Meynet G., Charbonnel C., Prantzos N., Ekström S., 2007, A&A, 464, 1029
- Gieles M., et al., 2018, MNRAS, 478, 2461
- Kroupa P., 2001, MNRAS, 322, 231
- Maoz D., Graur O., 2017, ApJ, 848, 25
- Marino A. F., et al., 2019, MNRAS, 487, 3815
- Milone A. P., et al., 2012, ApJ, 744, 58
- Nesaraja C. D., et al., 2001, Phys. Rev. C, 64, 065804
- Wang L., Kroupa P., Takahashi K., Jerabkova T., 2020, MNRAS, 491, 440
- Wirth H., Jerabkova T., Yan Z., Kroupa P., Haas J., Šubr L., 2021, MNRAS, 506, 4131
- Yan Z., Jerabkova T., Kroupa P., Vazdekis A., 2019, A&A, 629, A93
- Yan Z., Jeřábková T., Kroupa P., 2021, A&A, 655, A19
- de Mink S. E., Pols O. R., Langer N., Izzard R. G., 2009, A&A, 507, L1

Backup

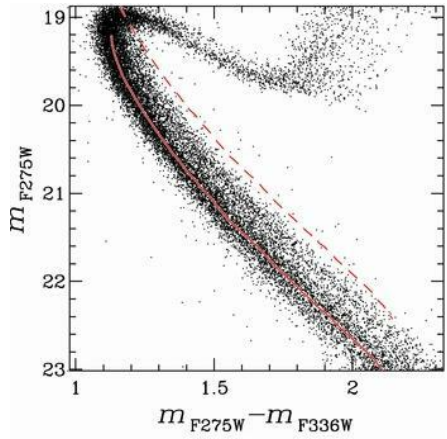


Figure: HR-diagram of the main sequence of 47 Tuc(Milone et al., 2012).

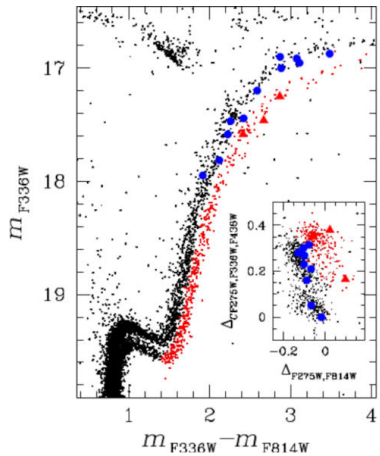


Figure: HR-diagram and Chromosome map of the red giant branch NGC 1851(Marino et al., 2019).

Backup

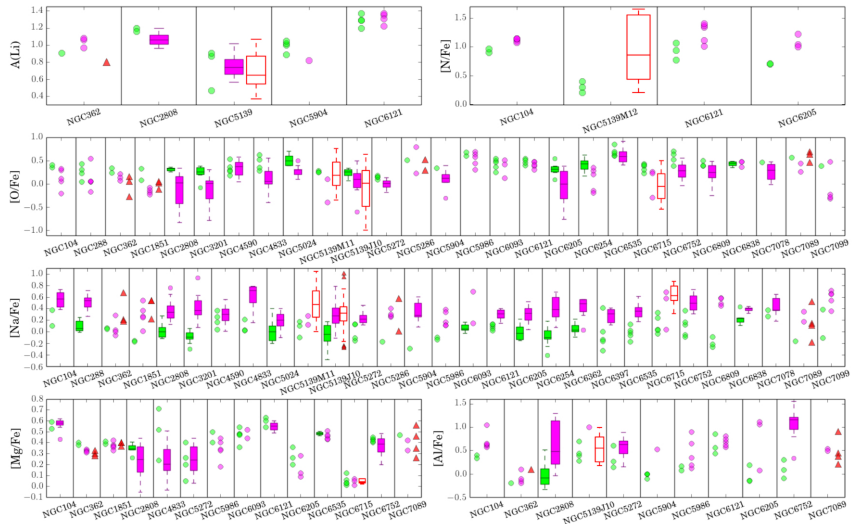


Figure: Different light element abundances for different GCs (Marino et al., 2019).

Backup

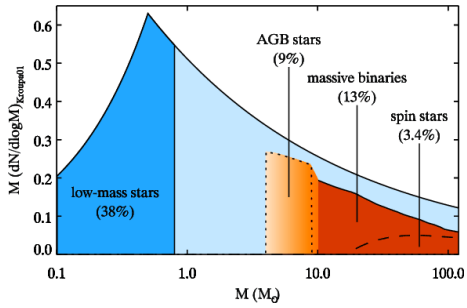


Figure: Different polluters and their mass fractions(Cottrell & Da Costa, 1981; Decressin et al., 2007; D'Ercole et al., 2008; de Mink et al., 2009; Wang et al., 2020).

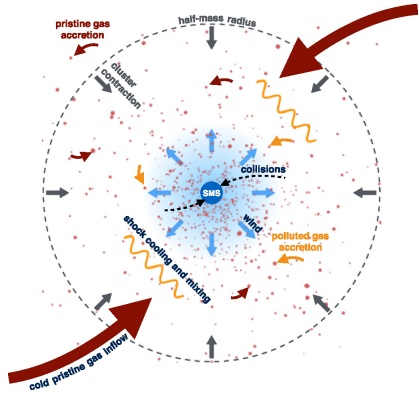


Figure: A supermassive star polluting the surrounding stars(Gieles et al., 2018)

Backup

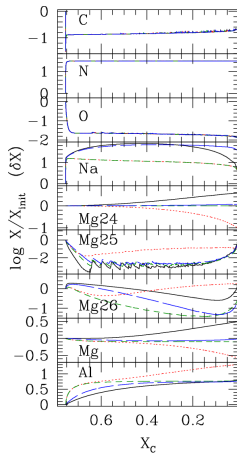
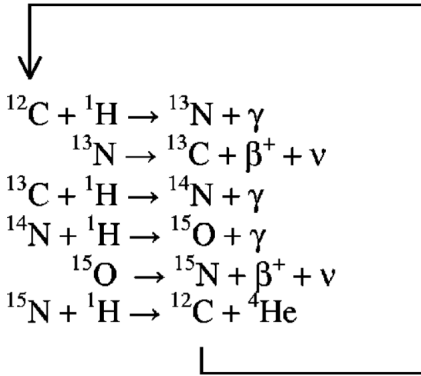


Figure: The CNO cycle (Nesaraja et al., 2001).

Figure: The evolution of central abundances in a $60 M_\odot$ rotating star (Decressin et al., 2007).

Backup

Baumgardt & Makino (2003); Wirth et al. (2021):

$$0 = \beta \left[\frac{\frac{M_{\text{ini}}}{\langle m \rangle}}{\ln(\gamma \frac{M_{\text{ini}}}{\langle m \rangle})} \right]^x \frac{R_{\text{ap}}}{\text{kpc}} (1 - e) \frac{1 - \frac{M(t)}{p_{SE} M_{\text{ini}}}}{\frac{t}{\text{Myr}}} - 1$$

$$p_{SE} = -0.61 + 0.52\alpha_3$$

Backup

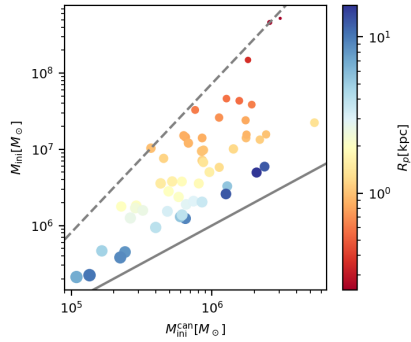


Figure: The initial masses computed using the canonical IMF compared to the ones assuming a top-heavy IMF (Wirth et al. 2022 in submission). The dashed grey line is

$$\frac{M_{\text{ini}}}{M_{\odot}} = 1.4 \times 10^{-4} \left(\frac{M_{\text{ini}}^{\text{can}}}{M_{\odot}} \right)^{2.0}.$$

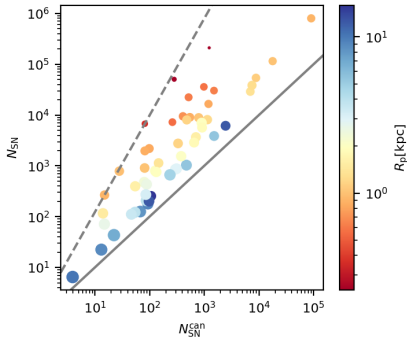


Figure: The initial masses computed using the canonical IMF compared to the ones assuming a top-heavy IMF (Wirth et al. 2022 in submission). The dashed grey line is $N_{\text{SN}} = 1.5 (N_{\text{SN}}^{\text{can}})^{1.9}$.

Backup

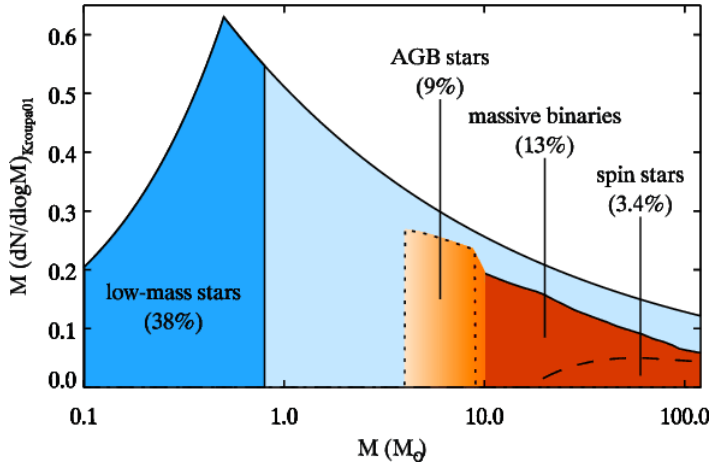


Figure: The IMF with different polluters and their mass fractions (Cottrell & Da Costa, 1981; Decressin et al., 2007; D'Ercole et al., 2008; de Mink et al., 2009; Wang et al., 2020).

Backup

Kroupa (2001)

$$dN = \xi(m)dm \quad \xi(m) = k_i m^{-\alpha_i}$$

$$\alpha_1 = 1.3,$$

$$0.08 \leq \frac{m}{M_\odot} \leq 0.5,$$

$$\alpha_2 = 2.3,$$

$$0.5 < \frac{m}{M_\odot}.$$

Backup

Yan et al. (2021)

$$dN = \xi(m)dm \quad \xi(m) = k_i m^{-\alpha_i}$$

$$\alpha_1 = 1.3 + Z_{\odot} \Delta \alpha (10^{[Z/H]_{\text{ini}}} - 1), \quad 0.08 \leq \frac{m}{M_{\odot}} \leq 0.5,$$

$$\alpha_2 = 2.3 + Z_{\odot} \Delta \alpha (10^{[Z/H]_{\text{ini}}} - 1), \quad 0.5 \leq \frac{m}{M_{\odot}} \leq 1,$$

$$\alpha_3 = \begin{cases} 2.3, & y < -0.87, \\ -0.41y + 1.94, & y \geq -0.87, \end{cases} \quad 1 < \frac{m}{M_{\odot}},$$

$$y = -0.14[Z/H]_{\text{ini}} + 0.99 \log_{10} \left(\rho_{\text{gas}} / (10^6 M_{\odot} \text{pc}^{-3}) \right).$$

Backup

Yan et al. (2021)

$$dN = \xi(m)dm$$

$$\xi(m) = k_i m^{-\alpha_i}$$

$$\alpha_1 = 1.3 + Z_{\odot} \Delta \alpha (10^{[\text{Z}/\text{H}]_{\text{ini}}} - 1),$$

$$0.08 \leq \frac{m}{M_{\odot}} \leq 0.5,$$

$$\alpha_2 = 2.3 + Z_{\odot} \Delta \alpha (10^{[\text{Z}/\text{H}]_{\text{ini}}} - 1),$$

$$0.5 \leq \frac{m}{M_{\odot}} \leq 1,$$

$$\alpha_3 = \begin{cases} 2.3, & y < -0.87, \\ -0.41y + 1.94, & y \geq -0.87, \end{cases}$$

$$1 < \frac{m}{M_{\odot}},$$

$$y = -0.14[\text{Z}/\text{H}]_{\text{ini}} + 0.99 \log_{10} \left(\rho_{\text{gas}} / (10^6 M_{\odot} \text{pc}^{-3}) \right).$$

Backup

Yan et al. (2021)

$$dN = \xi(m)dm$$

$$\xi(m) = k_i m^{-\alpha_i}$$

$$\alpha_1 = 1.3 + Z_{\odot} \Delta \alpha (10^{[\text{Z}/\text{H}]_{\text{ini}}} - 1),$$

$$0.08 \leq \frac{m}{M_{\odot}} \leq 0.5,$$

$$\alpha_2 = 2.3 + Z_{\odot} \Delta \alpha (10^{[\text{Z}/\text{H}]_{\text{ini}}} - 1),$$

$$0.5 \leq \frac{m}{M_{\odot}} \leq 1,$$

$$\alpha_3 = \begin{cases} 2.3, & y < -0.87, \\ -0.41y + 1.94, & y \geq -0.87, \end{cases}$$

$$1 < \frac{m}{M_{\odot}},$$

$$y = -0.14[\text{Z}/\text{H}]_{\text{ini}} + 0.99 \log_{10} \left(\rho_{\text{gas}} / (10^6 M_{\odot} \text{pc}^{-3}) \right).$$